TRANSPORT PROBLEMS 2018 Volume 13 Issue 3
PROBLEMY TRANSPORTU DOI: 10.20858/tp.2018.13.3.12

Keywords: simulation; crane; dynamics; FE analysis

Tomasz HANISZEWSKI
Silesian University of Technology, Faculty of Transport
Krasinski 8, 40-019 Katowice, Poland
Corresponding author. E-mail: tomasz.haniszewski@polsl.pl

STRENGTH ANALYSIS OF EXPERIMENTAL CRANE, USING PROLIFTOR 250 ROPE WINCH AS AN EXCITATION OF A GIRDER

Summary. The article presents the research carried out on the experimental construction of a crane, where a hoist with an AC motor without a motor control system was used as an excitation signal for the girder. The purpose of the described research is to determine the relationship between the values of the dynamic surplus factor when lifting the load with the loose rope in the initial phase of lifting and the distance of the hoist from the supporting structure. The data was obtained based on the force tests in a steel wire rope and subsequent determination of the values of stresses and deflections accompanying the selected test cases for different positions of the vibration inductor using the FE method.

1. INTRODUCTION

Overhead cranes are a means of transport that are very often found in all kinds of industrial plants. Due to the fact that her work is characterized by intermittent movement [1–6], there are some problems with this phenomenon. These problems include the susceptibility of the girder construction to vibrations and what is the danger of overloading the structure during incorrect operation or fatigue damage in selected locations of the structure. The purpose of this article is to present the construction and initial testing of a scaled model of a crane with particular emphasis on the lifting mechanism as an exciter and its impact on dynamic surplus factor when the lifting mechanism is in a different position on the girder. As it is mentioned earlier, the cranes are characterised by work with intermittent motion, the loads are therefore caused by the acceleration or deceleration of the work movement and are considered to be a regular load. Hence, lifting the load from the ground or releasing it causes vibration of the hoist structure [8–11, 13–18].

2. TEST OBJECT

The test object is a miniature overhead travelling crane with a total capacity of 80 kg. Table 1 shows the general characteristics of the tested overhead crane using PROLIFTOR 250 as a lifting mechanism.

Mechatronic models of cranes (fig. 1a) are a rare solution in relation to the objectives of research, especially the dynamics of the lifting mechanism.

Its main purpose is to study the dynamic behavior of the lifting mechanism when lifting the load, lifting load from the ground, lifting of frozen load, jerking due to the lack of control of the winding speed of the rope on the drum, dump of the mass or part of it, breaking and many other cases, which in varying degrees affect the coefficient of dynamic surplus factor. For this research, the lifting system consists of an AC (fig. 1b) motor without any controlling system for the determination of dynamic force values on the girder and wire rope.

Table 1

Characteristics of the experimental crane

description		symbol	dimension	value
lifting capacity		Q	[kg]	80
span		L	[m]	4
lifting height		$H_{p\,max}$	[m]	2
operating speed	lifting	v_h	[m/s]	0.16
	winch driving	v_{iw}	[m/s]	Without drive
supply voltage		U	[V]	220

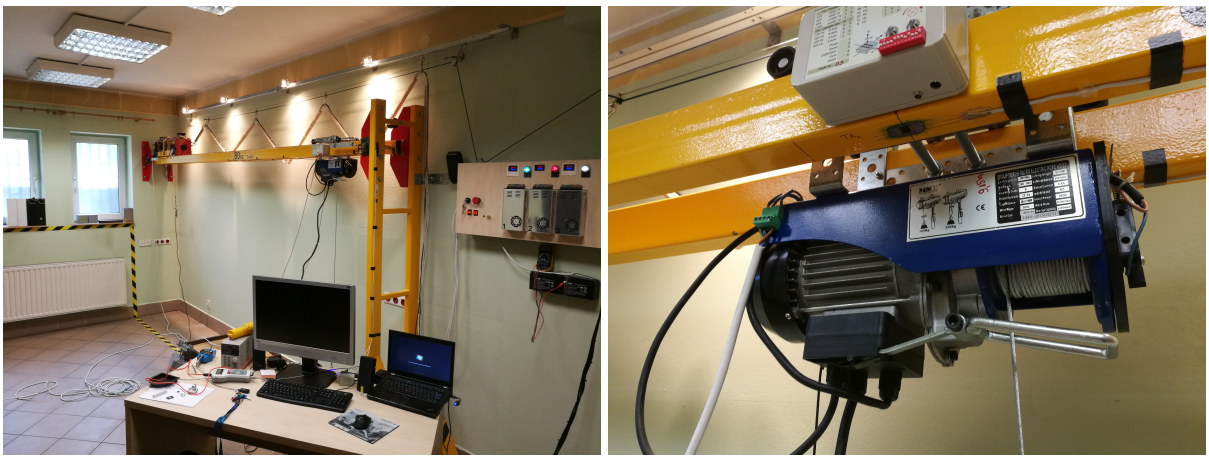

Fig. 1. The test stand: a) supporting structure with the power supply systems, b) vibration exciter PROLIFTOR 250

3. RESEARCH CARRIED OUT ON THE REAL OBJECT

During the tests, the construction was equipped with a vibration inductor based on a hoist PROLIFTOR 250 (fig.1b). The test was carried out for the loose rope case in the initial lifting phase, this process lasted until the engine was switched off by a mechanism limiting the lifting height. Then the load was lowered until the load hit the ground. Each measurement was performed 3 times. Figure 2 shows the research object with the location of measurement nodes marked as Node 3, Node 4, Node 2 – being acceleration sensors, Node 1 – being a force transducer. Acceleration measurements were made using a set of experimental wireless acceleration sensors based on the MPU6050 board (fig. 2, 3b), with resolution of 16 bit sampling frequency of 500 Hz for three measuring axes. The data were saved using the Bluetooth interface on a laptop computer. Measurement of the force in the rope was performed using a dynamometer FC2k AXIS (fig. 3a) equipped with an external force sensor. Measurements were recorded on the device memory card with a sampling frequency of 500 Hz.

The research plan included the measurement of accelerations in two positions of the vibration inductor i.e. 1 m and 2 m, respectively, from the support and force in the wire rope. In addition, the courses of force changes in the wire rope were recorded for the position of the vibration exciter, respectively, from 0.2 m to 2 m from the support in the step of 0.2 m.

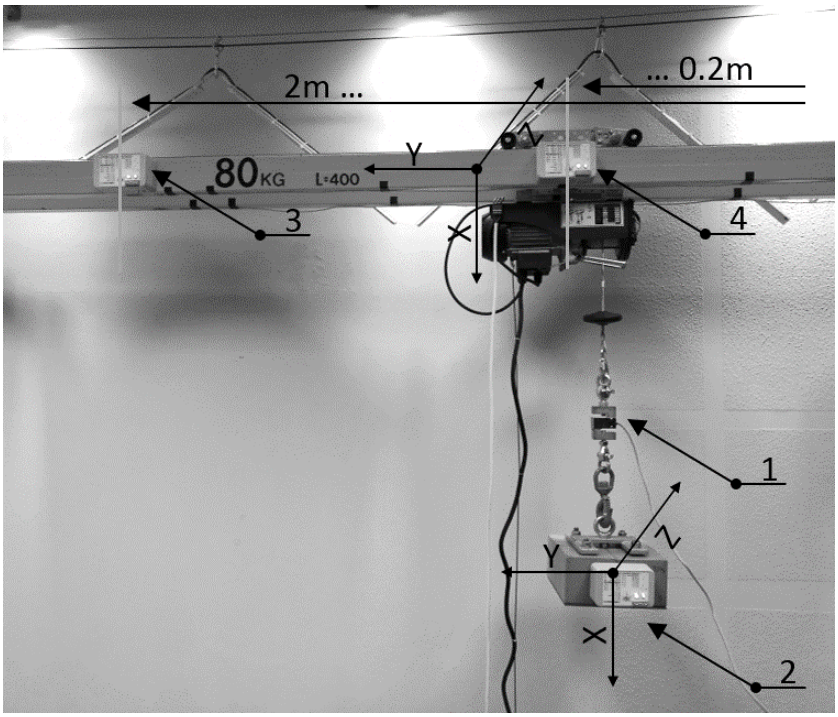

Fig. 2. Plan of distribution of measuring sensors: 1) force transducer, 2) acceleration measurement on the cargo – node 2, 3) measurement of acceleration on a girder at a distance of 2 m from the support – node 3, 4) measurement of acceleration at a distance of 1 m from the support – node 4

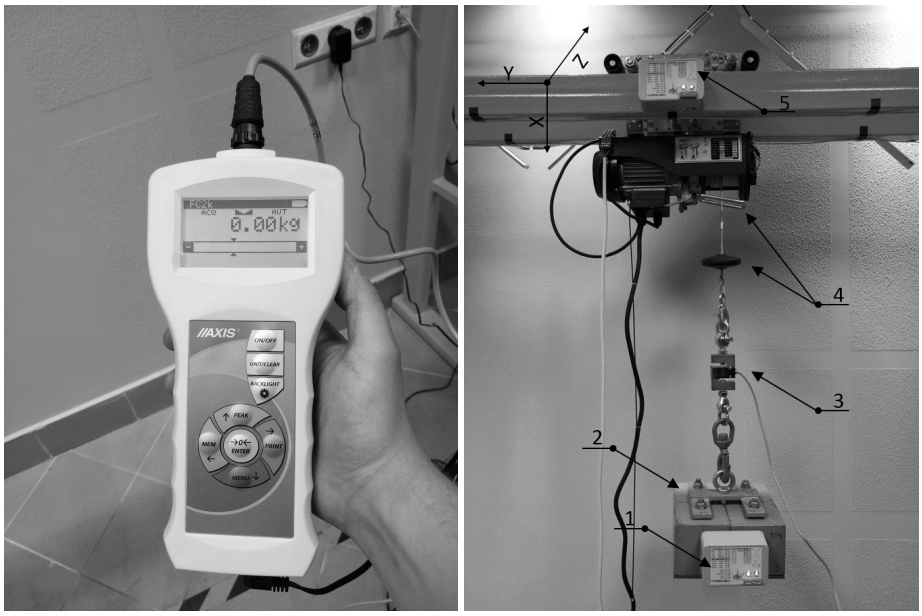

Fig. 3. a) Measuring the transducer AXIS cooperating with a force transducer 3, b) 1 – Node 2, 2 – cargo, 3 – force transducer 4 – lift height limiter, and 5 – node 4

4. RESULTS OF LABORATORY TESTS

As presented in the third point of this study, a series of tests were carried out on the discussed object, including the examined vibration of the girder. The first stage included measurements of forces in the wire rope and accelerations of selected spar points, with the position of the vibration inductor at a distance of 1 m and 2 m from the main support. The time series of force changes in wire rope are shown in figures 4 and 5.

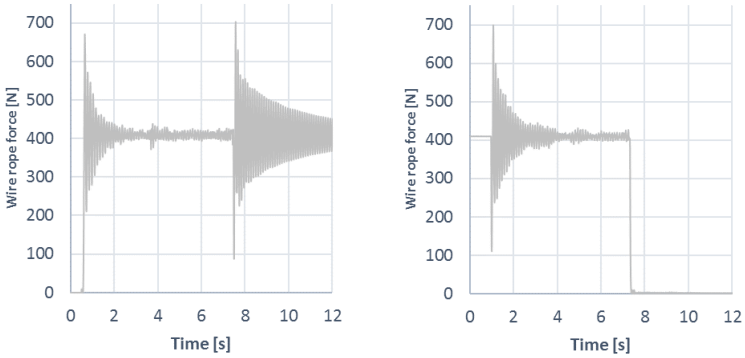

Fig. 4. Force in the wire rope: a) lifting, b) lowering for L_w=1 m, where L_w – the distance of the inductor from the support

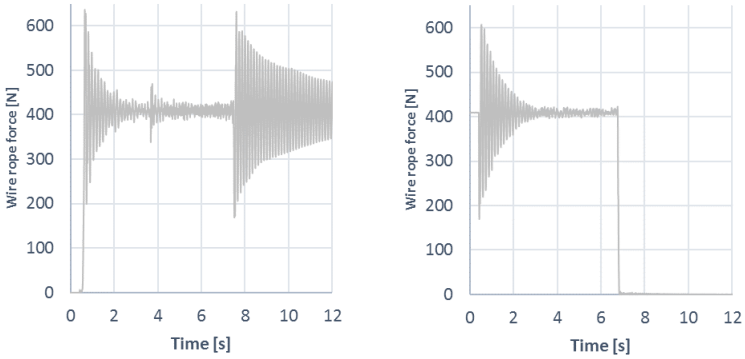

Fig. 5. Force in the wire rope: a) lifting, b) lowering for L_w=2m, where L_w – the distance of the inductor from the support

As can be observed, the values of dynamic forces in the case of the position of the vibration exciter are closer to the support, and therefore in a place with higher stiffness causes a significant increase in forces (Fig. 4a).

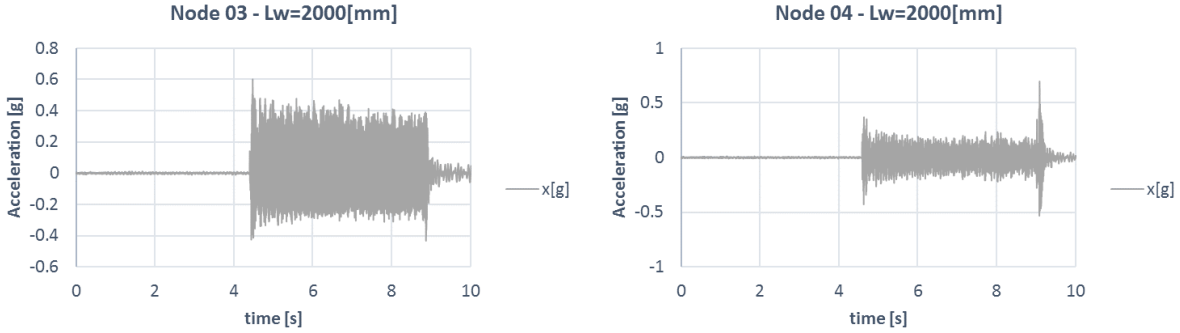

Fig. 6. Acceleration waveforms in node 4, three for cases where the load is missing, successively lifting, and lowering for L_w=2m, where L_w—the distance of the inductor from the support

In the case of placing the vibration exciter in the middle of the span, i.e., the more susceptible, these forces are slightly smaller (fig. 5). In figs. 4 and 5, you can also observe significant values of forces caused by the impact of the lifting limiter by the limit switch. This phenomenon is visible in figs. 4 and 5 in the 8th second of measurement. Similarly, when lowering, a sudden engine start causes a significant oscillation of the dynamic force in the tested wire rope.

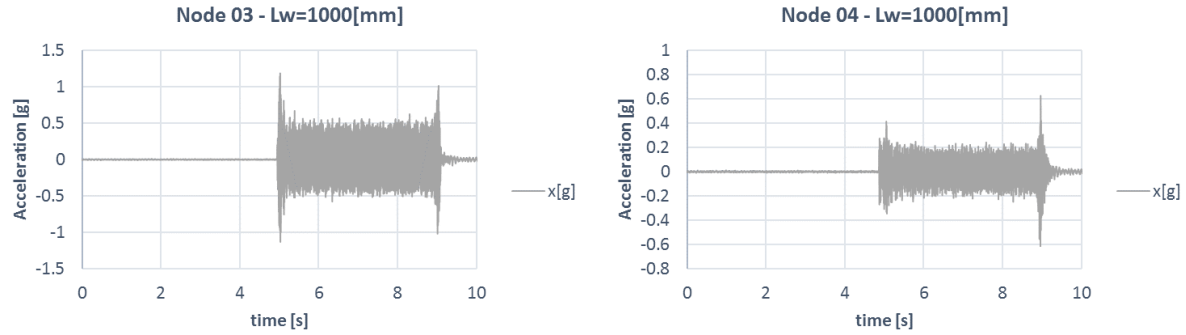

Fig. 7. Acceleration waveforms in node 4, three for cases where the load is missing, successively lifting, and lowering for L_w=1 m, where L_w – the distance of the inductor from the support

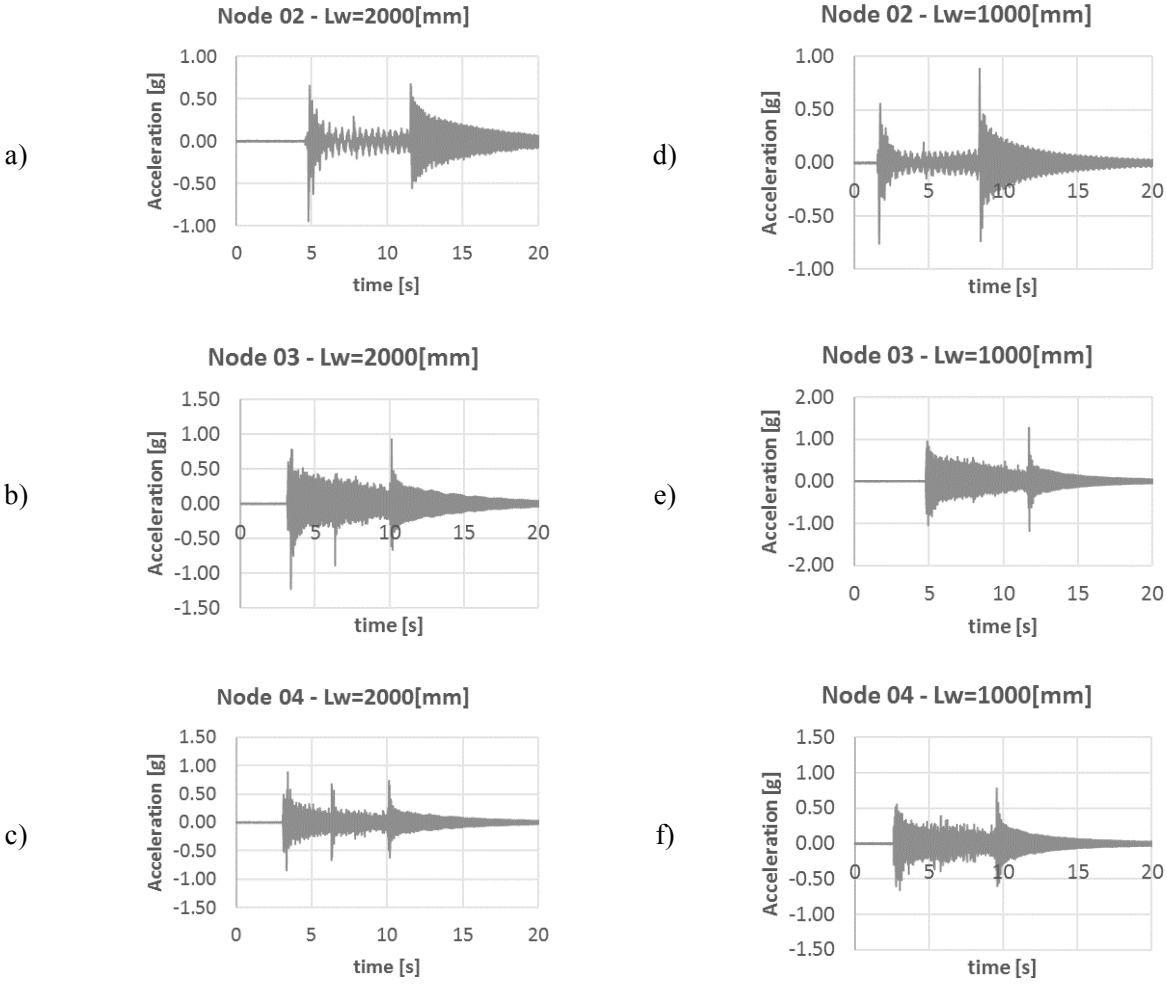

Fig. 8. List of waveforms of accelerations in nodes 4, 3, and 2 for cases where the load is 42 kg, lifting and lowering cycle for L_w=1 m and 2 m for lifting axis, where L_w – the distance of the inductor from the support

For the considered case, the values of accelerations were also verified in three measuring axes. In the case of lifting an empty hook (fig. 7), the acceleration values oscillate at the limit of -0.42g to 0.59g for the vibration inductor located at a distance of 2 m from the support, and the measurement was made at the same point. For the same position of the vibration inductor, the values of accelerations at a distance of 1 m from the support range from -0.42g to 0.34g, therefore they are similar.

For the case of locating the vibration exciter at a distance of 1 m from the support, the values of accelerations at a distance of 1 m from the support are already -1.12g to 1.17g, -0.34g to 0.37g for measurement at a distance of 2 m from the support, and are three times smaller than the value in the middle of the girder. These vibrations are caused mainly by the movements of the vibration exciter. These results are shown in figures 6 and 7.

The next considered case was the lifting of the test load weighing 42 kg. The load was lifted in the most unfavourable way, i.e., without the pre-tension of the steel wire rope subsequently for L_w = 2m and L_w = 1m. Figure 8 shows the acceleration values for three measuring points, Node 2 on the load, Node 3 at a distance of 1 m from the support, and Node 4 at a distance of 2 m from the support. Figure 8 presents a summary of the results obtained, i.e., minimum and maximum values only in the case of load jerk. In addition, in fig. 8, the stroke of the height limiter of the lifting mechanism and the impact on the ground can be observed successively.

A comparison of the results obtained on the basis of figure 10 is shown in table 2.

Table 2

List of acceleration values for considered research cases in the lifting axis

Excitation placement	Measurement node	Min. Acceleration value [g]	Max. Acceleration value [g]
	Node 2	-	-
Empty - L_w=1m	Node 4	-0.34	0.37
	Node 3	-1.12	1.17
	Node 2	-	-
	Node 4	-0.42	0.34
Empty - L_w=2m	Node 3	-0.42	0.59
	Node 2	-0.76	0.55
Loaded - L_w=1m	Node 4	-0.65	0.55
	Node 3	-1.02	0.82
	Node 2	-0.94	0.56
	Node 4	-0.83	0.88
Loaded - L_w=2m	Node 3	-1.21	0.65

As can be seen in table 2 and figure 8, the location of the vibration exciter in close proximity to the support results in large amplitudes of vertical vibrations reaching from -1.21g to 0.82g in the middle of the span of the girder.

Table 3

Values of forces and dynamic overloads in the wire rope for considered research cases

L_w [m]	0.2	0.4	0.6	0.8	1.0	1.2	1.4	1.6	1.8	2.0
F_{max} [N]	747.0	749.0	745.1	683.3	686.7	664.6	671.0	637.2	614.1	641.7
F_{stat} [N]	407.4	406.1	407.1	407.1	406.0	405.9	405.4	405.6	406.3	406.1
φ_2 [N]	1.83	1.84	1.83	1.66	1.69	1.64	1.65	1.57	1.51	1.58

Table 3 presents the results of the last of the tests, i.e., the values of forces in the wire rope, both static and dynamic, allowing to determine the ratio of the dynamic surplus factor in the wire rope. Values were collected for locating the vibration exciter at 0.2 m steps up to the center of the girder.

5. STRENGTH CALCULATIONS OF THE CRANE STRUCTURE

In order to carry out calculations using the FE method, the geometric model of the tested structure was used based on the construction documentation made for the purpose of building the presented test stand. The model was entirely made in the Autodesk Inventor program.

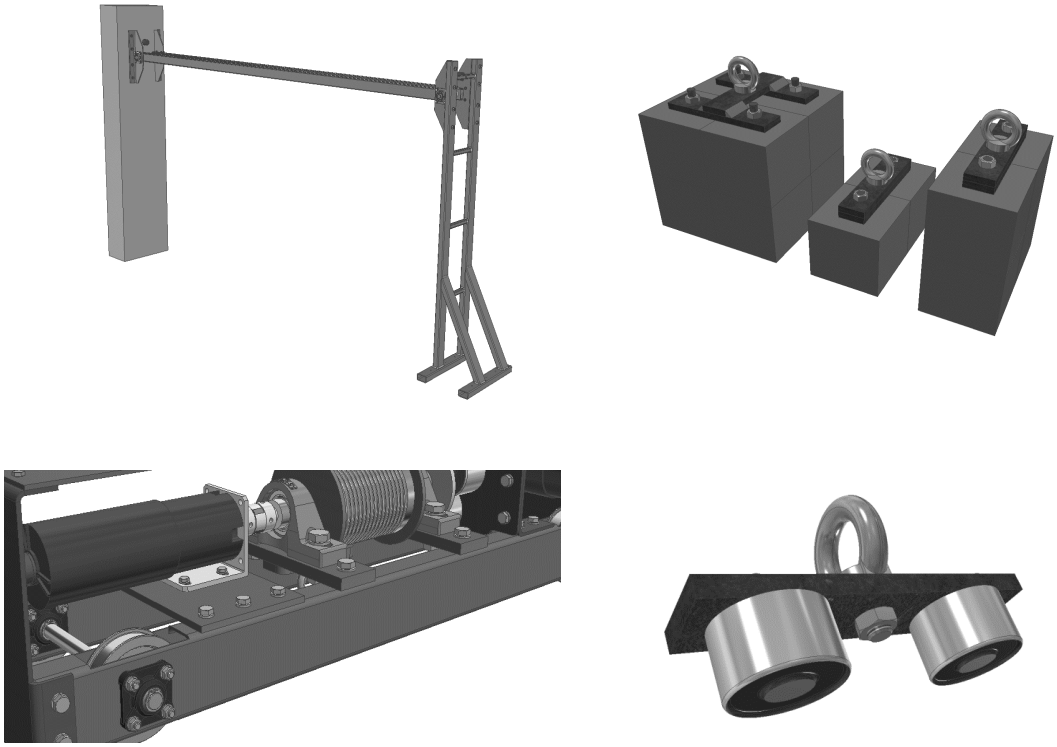

Fig. 9. 3D model of: a) an experimental test stand, b) set of test loads, c) a trolley with lifting and driving mechanism, and d) electromagnetic grip

Figure 9 is a supporting structure, trolley with lifting and driving mechanism, and an electromagnetic grip. The tested girder is a thin-walled structure in which one of the dimensions (thickness) is significantly smaller than others. Such structure is often called the surface girder, which is characterized by a high load carrying capacity. In the case of the structure being tested, the ratio of the length of individual sheets to their thickness is significantly less than one, which unambiguously confirms that the tested structure should be treated as the surface, making the discrete model mainly composed of shell-type SHELL elements.

In order to determine the stiffness, deflection, or stress of the structure, a FE model of the tested crane was built, which allows to carry out calculations. For the construction of a discrete model, shell elements S3 and S4 and beam element B31 were used. On the surface model, conventional shell elements, SHELL S3 and S4, of the first order with an average size of 8 mm were generated. These elements are defined on the reference surface, being a separate middle surface. The properties of a given group of elements are defined by assigning to the section. As a result of the discretization, a grid consisting of 187651 elements was obtained. These elements were assigned sections taking into account the thickness of individual sheets of the structure and the material from which they were made. The construction of the research test bench is made of elements made mainly of S235 steel. The following material properties are assigned to the respective groups of elements in the appropriate sections (table. 4).

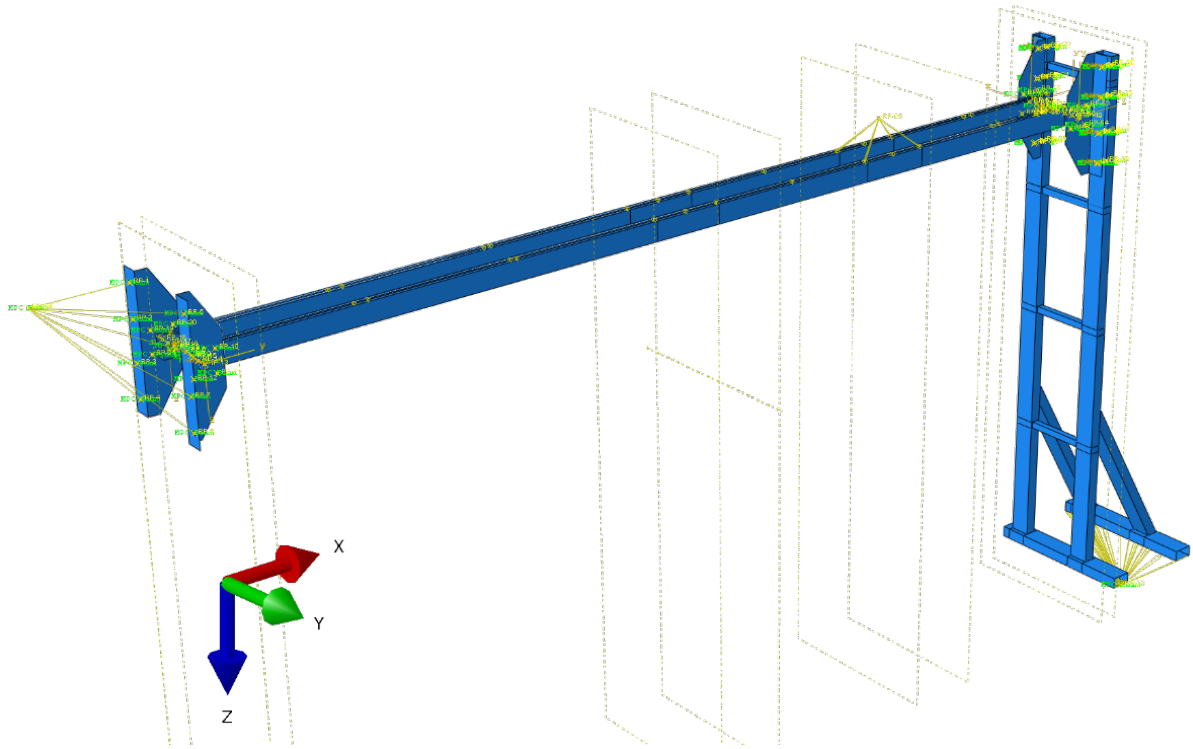

Fig. 10. FE model of the research object

Table 4

Material data S235 [7]

Poisson's coefficient for steel	ν	0.3[-]
Young's modulus for steel	E	210000[MPa]
Density of steel	ρ	7.86e-9[ton/mm^3]
Kirchhoff module for steel	G	81000[MPa]

The bolt joints connecting the girder brackets were modeled as beam elements of the MPC BEAM type (figs. 10 and 11), connecting them to the structure by DISTRIBUTING COUPLING elements. Then, the movable connection in the design is realized by a set of bearings; they are realized in the FE model with elements of the MPC BEAM casting axis, and the connection type of hinge giving the possibility of carrying out a rotation about its axis and the same axis is connected with holes in the girder by means of the MPC BEAM.

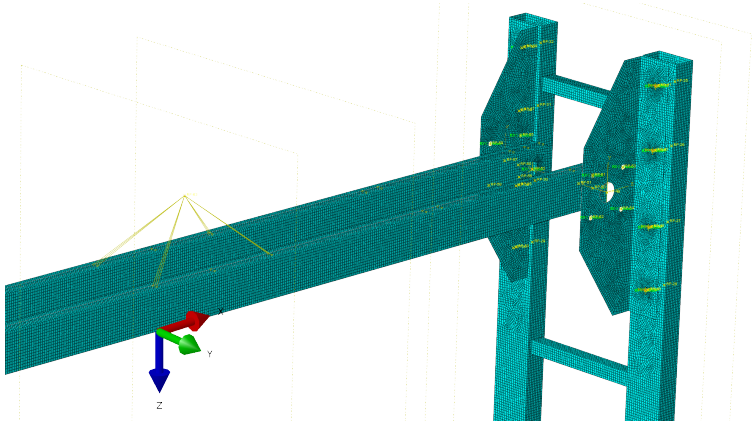

Fig. 11. FEM model or research object – plan of used couplings and constraints

The load was applied using DISTRIBUTING COUPLING CONSTRAINT elements, guaranteeing an even load distribution on the rail.

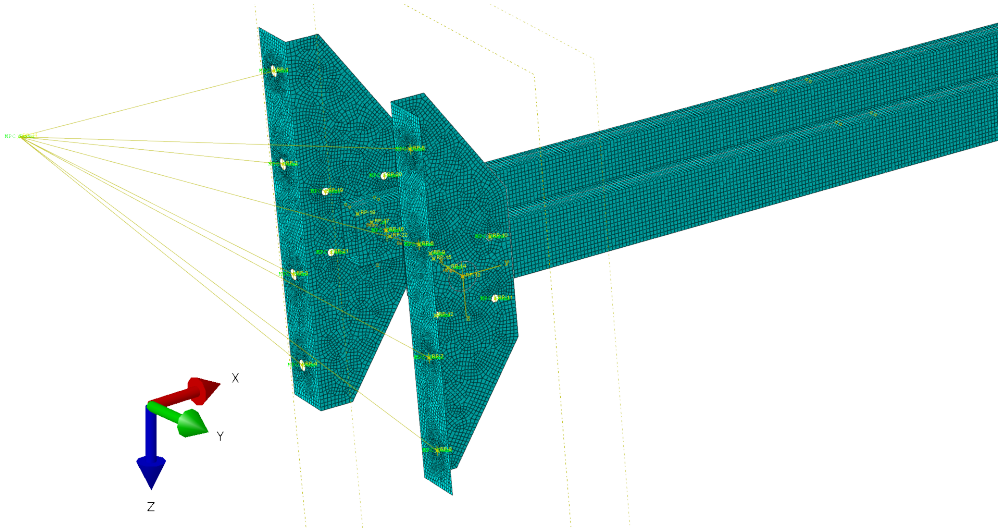

Fig. 12. FEM model or research object – plan of used couplings and constraints

The movable bracket of the girder and the supporting frame were fixed with a rigid DISTRIBUTING COUPLING element (fig. 12), giving boundary conditions at the location of the main node. In the discussed nodes, all degrees of freedom were received in both supports (figs. 11 and 12). The calculation process has been divided into several phases. The first one included verification of deflection and stress at no load. Then, the structure was loaded with a static and dynamic working load determined on the basis of laboratory tests in two selected positions, i.e., 1 m and 2 m from the support. The simulation results are shown below.

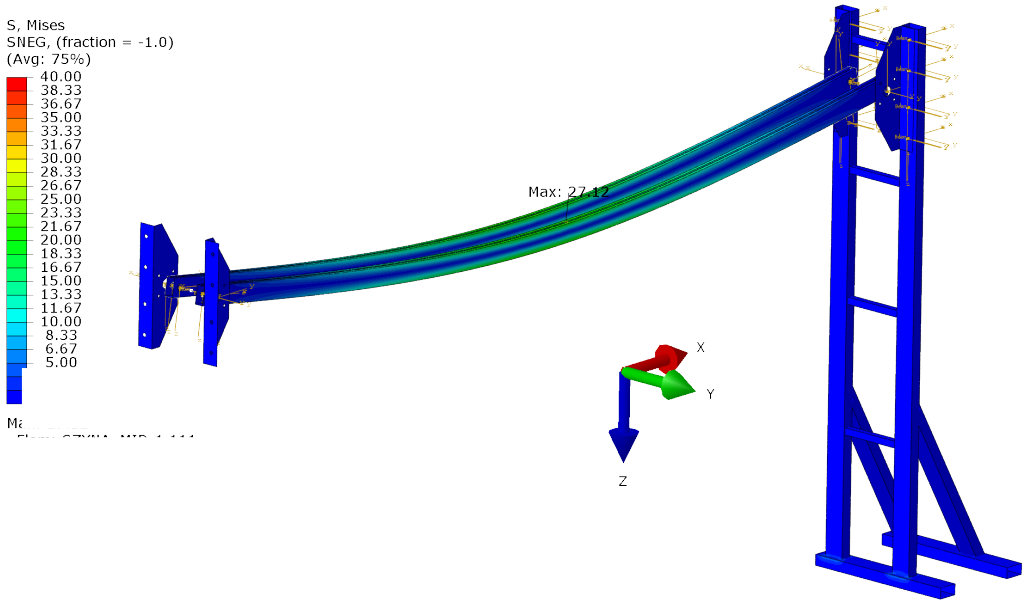

Fig. 13. The influence of the own weight and cargo load in the distance L_w=2m – static value, stresses reduced according to the Huber–Mises–Hencky theory

The values of received stresses in the girder are presented in Table 5 and figs. 13 and 14 for static and dynamic cases.

Table 5

The results of numerical analysis

Load Case			Load Name	φ_{2rope} [-]	U [mm]	S [MPa]	$\varphi_{2girder}$ [-]
Gravity			Static - L100	1.00	1.33	7.36	1.00
Gravity			Static - L200	1.00	1.33	7.36	1.00
Gravity +	536.61	N	Static - L100	1.00	3.08	21.32	1.00
Gravity +	536.61	N	Static - L200	1.00	3.89	27.12	1.00
Gravity +	912.35	N	Dynamic - L100	1.66	4.31	32.33	1.52
Gravity +	868.38	N	Dynamic - L200	1.58	5.48	39.64	1.46

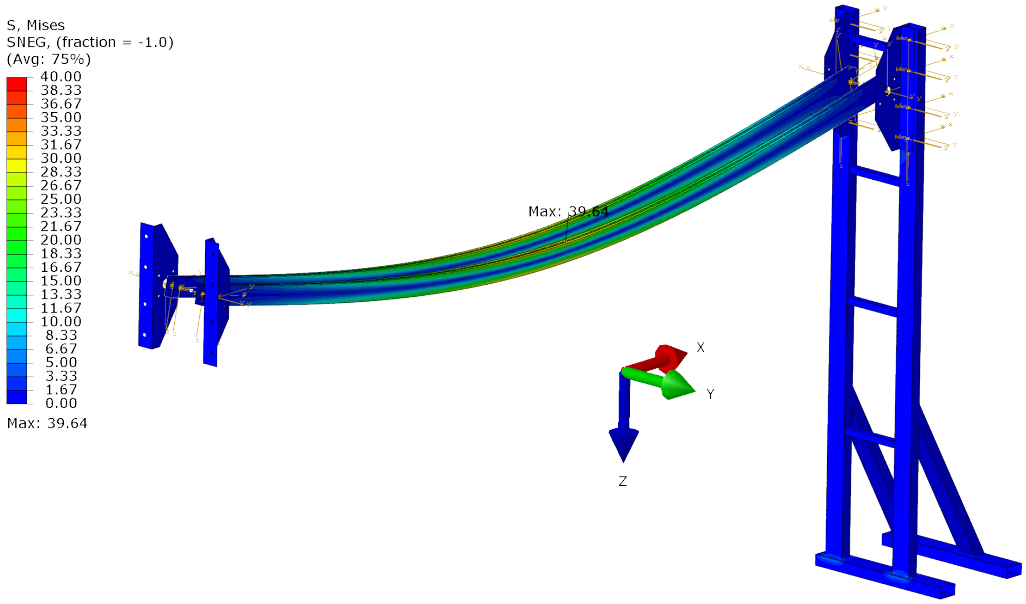

Fig. 14. The influence of the own weight and cargo load in the distance L_w=2m – dynamic value, stresses reduced according to the Huber–Mises–Hencky theory

As can be seen in Table 5, the stress values caused by the load pickup generate the surplus coefficient factor of a smaller value. They have a ratio of 1.09 in both cases.

6. CONCLUSIONS

The simulation tests carried out in this article with the use of FEM were preliminary tests, where the obtained results in the form of deflections and stresses will be used in simulation studies of the lifting mechanism of the crane.

a)

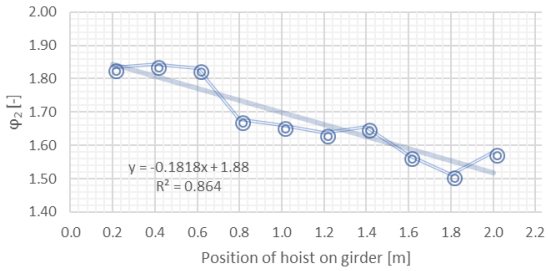

b)

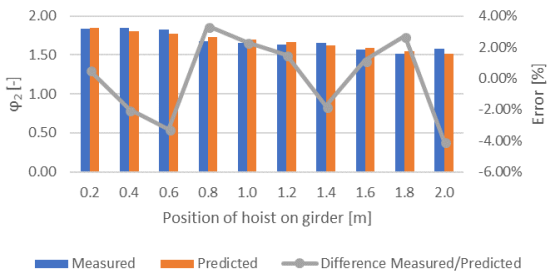

Fig. 15. Values of the dynamic surplus coefficient: a) measured values, and trend function, b) comparison of the measured and expected values and differences between them

The presented FE model can be the basis for further research, so-called hybrid approach that combines a dynamic model with the FE model. This solution allows to identify the state of stress and strain during dynamic loads as well as to evaluate vibrations at any chosen place in the structure. Lifting the load, unrelated to the ground is, as presented, the source of mechanical vibrations of structures of various intensity. Depending on the elastic properties of the girder and the dynamics of lifting mechanism, the design of the hoist requires taking into account the dynamic factor of inertia and gravity influencing the elevated load not connected to the ground. The values of coefficient φ_2 are determined on the basis of the dependence given in the norm [5, 12].

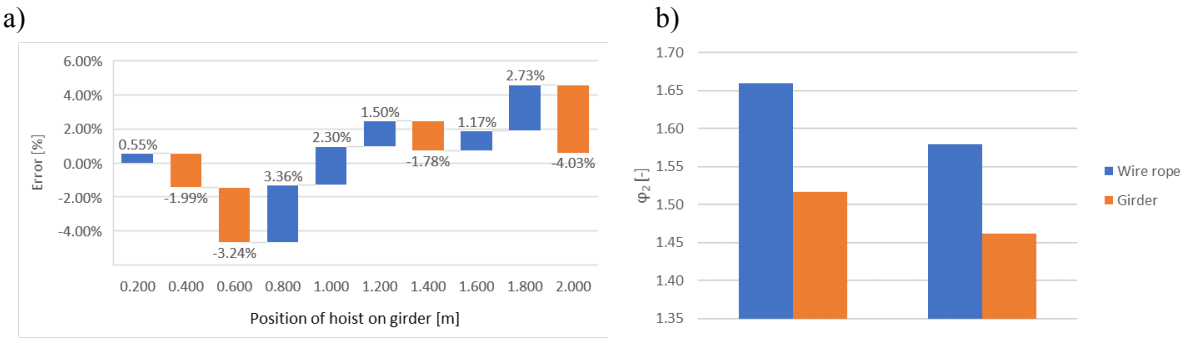

Fig. 16. Values of the dynamic surplus coefficient a) percentage differences between the measured value and the predicted value in relation to the position of the vibration exciter on the girder, b) differences between the dynamic value in the rope and the girder

On the basis of the conducted research, it should be taken into account the fact that the value of dynamic surplus factor in the wire rope is about 10% greater than in the girder (fig. 16b) for the tested case, which is caused, among other things, by the rope construction itself and its properties to damp vibrations. It should also be remembered that this difference may be different for different types of construction and will depend on the length of the rope.

Using the simple linear trend function (fig. 15a), a function describing the distribution of the dynamic coefficient along the span of the girder can be obtained. In the given case, the values of the dynamic force in the rope can be said to change almost linearly, and the dynamic lifting factor decreases in the rope as the span's girder approaches the center (fig. 15), where it is most susceptible to the forces generating the bending moment and high stresses. According to the obtained trend function, errors between predicted and received values based on measurements are within the 4% limit (fig. 16a).

References

1. Bogdevičius, M. & Vika, A. Investigation of the dynamics of an overhead crane lifting process in a vertical plane. *Transport.* 2005. 20(5) p. 176-180.
2. Haniszewski, T. Modeling the dynamics of cargo lifting process by overhead crane for dynamic overload factor estimation. *J. Vibroeng*. 2017. Vol. 19. Iss. 1. P. 75-86.
3. Kosucki, A & Malenta, P. The possibilities of reducing the operational load of hoisting mechanisms in case of dynamic hoisting. *Maintenance and Reliability.* Vol. 18(3). June 2016. P. 390-395.
4. Markusik, S. & Gąska, D. & Witaszek, K. Badania przyspieszeń i poziomów drgań w suwnicach pomostowych. *Scientific Journal of Silesian University of Technology. Series Transport*. 2007. Vol. 63. P. 181-186. Wydawnictwo Politechniki Śląskiej. Gliwice. [In Polish: Study of acceleration and vibration levels in bridge cranes].

5. Margielewicz, J. & Haniszewski, T. & Gąska, D. & Pypno C. *Badania modelowe mechanizmów podnoszenia suwnic.* Katowice: Polish Academy of Science. 2013. [In Polish: *Model studies of cranes hoisting mechanisms*].
6. Oguamanam, D.C.D. & Hansen, J.S. & Heppler, G.R. Dynamic response of an overhead crane system. *Journal of Sound and Vibration.* Vol. 213. No. 5. 1998. P. 889-906.
7. Piątkiewicz, A. & Sobolski, R. *Dźwignice*. WNT. Warszawa, 1978. [In Polish: *Cranes*].
8. Reutov, A.A. & Kobishchanov, V.V. & Sakalo, V.I. Dynamic Modeling of Lift Hoisting Mechanism Block Pulley. *Procedia Engineering.* Vol. 150. 2016. P. 1303-1310.
9. Savković Mile M. & Radovan, R. & Bulatović, Milomir M. & Gašić, Goran V. & Pavlović, A. & Stepanović, Z. Optimization of the box section of the main girder of the single-girder bridge crane by applying biologically inspired algorithms. *Engineering Structures.* Vol. 148. 2017. P. 452-465.
10. Wu Jia-Jang Transverse and longitudinal vibrations of a frame structure due to a moving trolley and the hoisted object using moving finite element. *International Journal of Mechanical Sciences*. Vol. 50. No. 4. 2008. P. 613-625.
11. Zrnić, N.Đ. &. Gašić, V.M. & Bošnjak, S.M. Dynamic responses of a gantry crane system due to a moving body considered as moving oscillator. *Archives of Civil and Mechanical Engineering.* Vol. 15. No. 1. 2015. P. 243-250.
12. PN-EN 13001-2:2013. *Bezpieczeństwo dźwignic. Ogólne zasady projektowania. Część 2: Obciążenia.* Warszawa: Polski Komitet Normalizacyjny. [In Polish: *Security of cranes. General principles for design. Part 2: Loads.* Warsaw: Polish Committee of Standardization].
13. REN Hui-li, WANG Xue-lin, HU Yu-jin, and LI Cheng-gang. Dynamic Response Simulation of Lifting Load System of Ship-mounted Cranes. *Journal of System Simulation.* 2007. Vol. 19. No. 5. P. 2665-2668.
14. Chen Huixian & Liu Shuang & Tang Qingtai. Dynamics Simulation and Analysis on Wire Rope of a Mine Hoist Based on SIMULINK. *Mining & Processing Equipment.* 2008. Vol. 36(9). P. 44-47.
15. Gąska, D. & Margielewicz, J. & Haniszewski, T. & Matyja, T. & Konieczny, Ł. & Chróst, P. Numerical identification of the overhead travelling crane's dynamic factor caused by lifting the load off the ground. *Journal of Measurements in Engineering.* 2015. Vol. 3(1). P. 1-8.
16. Gąska, D. & Haniszewski, T. Modelling studies on the use of aluminium alloys in lightweight load-carrying crane structures. *Transport Problems*. 2006. Vol. 11(3). P. 13-20.
17. Oguamanam, D.C.D. & Hansen, J.S. &. Heppler, G.R. Dynamic response of an overhead crane system. *Journal of Sound and Vibration*. 1998. Vol. 213(5). P. 889-906.

Received 09.12.2016; accepted in revised form 10.09.2018